

Classification of states of low-frequency systems of geophysical monitoring

A. A. Lyubushin Jr.

Institute of Experimental Geophysics of UIFE, Russian Academy of Sciences, Moscow

Introduction

This paper continues a previous study [Lyubushin, 1993] and is devoted to questions of multidimensional processing of time series in geophysical monitoring systems. The principle application of the proposed algorithms is low-frequency monitoring systems with operating periods ranging from several minutes and higher up to several hundreds of hours. (The upper bound of the period depends on the duration of observation.) Appropriate systems include earthquake prediction and control over large engineering structures and the ecological environment. The main difficulty in time series processing of low-frequency monitoring is an absence or extreme broadening of the “event,” i.e., a sharp change of amplitude and frequency composition of a recorded signal. For an example of different ranked seismic nets, the principle purpose of observation and data processing is discrimination and classification of seismic events. The time series obtained from low-frequency systems (for example, a strainmeter net or the net of spaced boreholes with synchronous logging of underground water levels) are characterized by a broadband power spectrum increasing with decreasing frequency ω by the law $\omega^{-\beta}$, $\beta = 1.5 - 2.5$, and having no specific features except for possible monochromatic components corresponding to diurnal and half diurnal harmonics of the tidal deformations of the crust and to temperature variations (the diurnal temperature changes can generate a “comb” of harmonics with the frequencies of $n/24$ hours $^{-1}$, $n = 1, 2, 3, \dots$).

Such a “gray” behavior of the recorded signal leads to a loss of significance for measurements of only one type low-frequency background processes in one observation point for solution of many geophysical problems (e.g., earthquake prediction). The situation reverses if the number of observation points increases or the number of measured values increases, since in these cases it is possible to use cross spectral, instead of two one-dimensional analysis, and for more than observation points to use spectral matrix analysis of multidimensional series.

Similar analysis allows discrimination of the new (compared with the conventional bay-like anomalies in seismic regions) signal: enhancement of synchronous or collective behavior either by spacing transducers of the monitoring system or by measuring physically different processes at one site within the frequency bands and time intervals in which such synchronization is observed.

Lyubushin [1993] proposed to use the principle component method in the frequency domain [Brillindjer, 1980] for discrimination of the synchronizing effect. From the computational point of view, this method estimates the largest eigenvalue $\lambda_1(\omega)$ of the spectral matrix $S(\omega)$. This eigenvalue is the power spectrum of the first principle component of an initially multidimensional series, i.e., some scalar time series that can be obtained by linear filtration of the initial series and that contains maximal information on simultaneous (synchronous) behavior of the linear combination of scalar components of the initial Gaussian vector series [Brillindjer, 1980]. An increase in the value of $\lambda_1(\omega)$ in definite frequency bands implies increasingly synchronous behavior of the harmonic constituents from these bands for all scalar components of the initial vector series.

If now the greatest eigenvalue $\lambda_1(\omega)$ of the spectral matrix $S(\omega)$ is estimated in a sliding time window with readings of fixed length L rather than over all sampling, then we obtain two-parameter dependence $\lambda_1(\tau, \omega)$ where τ is the window time coordinate, for example, the time corresponding to the right-hand termination of the window. The dependence $\lambda_1(\tau, \omega)$ can be represented in the form of level curves or spatial surfaces, and the jumps in λ_1 values will be in line with the time intervals τ and frequency bands in which the synchronous behavior of the scalar components of the initial multidimensional time series is most pronounced. It is this procedure that was proposed and programmed in the work by Lyubushin [1993], where, in addition, the estimation of the matrix $S(\omega)$ was conducted by non-parametric methods using frequency-averaged multidimensional periodograms. Thus the method proposed by Lyubushin [1993] is conceptually an extension of common one-dimensional time spectral analysis (STA) to the multidimensional case.

One of the features of low-frequency geophysical monitoring systems is the physical nonuniformity of time series obtained from the same or various measurement points. For example, the underground water level is measured in one place the strains in another place and the seismoacoustic emission intensity in a third place. The constraints are frequently simultaneous one-point measurements of several physically unlike quantities of different dimensions and variation ranges. Despite their nonuniformity and scale differences they are integrated into a general data set, since all measurements are conducted simultaneously and reflect, at least in some measure, the processes occurring in the Earth's crust. Therefore of interest for very different types of monitoring problems is the detection of the collective behavior of experimental results for various geophysical fields within the limitations of the frequency bands and time intervals where this behavior is observed. However, in doing so we need to circumvent the influence of scale differences of the scalar components of the initial vector time series. Furthermore, since evaluation of the spectral matrix $S(\omega)$ is made in the sliding time window, i.e., over comparatively short samples, eliminating the dominant effects of the low frequencies makes discretization appropriate before estimation of $S(\omega)$ in each window. To remove the effects of multiplexing, each scalar component of the vector series should be normed by the unit sampling dispersion [Lyubushin, 1993]. These preliminary procedures realize spectral matrix normalization of a sort in each time window and enable physically nonuniform information to be processed.

In this paper, I briefly describe the parametric realization of the estimation algorithm $\lambda_1(\tau, \omega)$, argue for the use of estimates of $\lambda_1(\tau, \omega)$ in cases when there are no distinct jumps in the values of the first eigenvalue, and give examples of real data processing.

Parametric Estimate of $\lambda_1(\tau, \omega)$

Let $\mathbf{X}(t) = (X_1(t), \dots, X_m(t))^T$, $t = 1, \dots, L$ be sampling of an initially multidimensional time series in any window with the length of L readings (for the sake of definiteness the first window is assumed). Here, m is the dimension of the column vector $\mathbf{X}(t)$, t is discrete time (numbering of the sequential readings), and T denotes transposition. For brevity, we sometimes drop the argument τ specifying the time window.

Converting to a series of differences (increments)

$$\mathbf{x}(t) = \mathbf{X}(t+1) - \mathbf{X}(t), \quad t = 1, \dots, L-1 \quad (1)$$

for each component $x_i(t)$, $i = 1, \dots, m$, we calculate sampling estimates of the mean s_i and dispersion σ_i in the moving window

$$s_i = \sum_{t=1}^{L-1} x_i(t)/(L-1) \quad (2)$$

$$\sigma_i^2 = \sum_{t=1}^{L-1} (x_i(t) - s_i)^2/(L-2)$$

and norm each component by unit dispersion

$$x_i(t) := (x_i(t) - s_i)/\sigma_i, \quad i = 1, \dots, m \quad (3)$$

Further, we need to construct an estimate of the spectral matrix $S(\omega)$. Experience shows that the nonparametric estimate used by Lyubushin [1993] (through the Fourier transform with respect to samplings in each window and frequency averaging of multidimensional periodograms) at small values of L has insufficient frequency resolution. Therefore we prefer below the parametric estimate with the use of the multidimensional autoregressive model [Marple, 1990]

$$\mathbf{x}(t) + \sum_{k=1}^p A_k \mathbf{x}(t-k) = \vec{\varepsilon}(t) \quad (4)$$

where $p \geq 1$ is the order of the autoregression, A_k , $k = 1, \dots, p - (m \times m)$ are the autoregressive coefficient matrices, and $\vec{\varepsilon}(t)$ is the m dimensional series of identification residuals which is assumed to be the sequence of independent Gaussian vectors with zero mean and covariation matrix \mathbf{P} .

To determine the matrices \mathbf{P} and A_k , $k = 1, \dots, p$ we apply the multidimensional Darbin-Levinson procedure requiring preliminary estimates of the covariance $(m \times m)$ matrices

$$R(k) = \langle \mathbf{x}(t+k) \mathbf{x}^H(t) \rangle, \quad k = 0, 1, \dots, p$$

where $\langle \dots \rangle$ is the time-averaging symbol and H is the Hermitian conjugate superscript [Marple, 1990].

Having determined the matrices \mathbf{P} and A_k , $k = 1, \dots, p$ we estimate the complex spectral matrix $S(\omega)$ from the formula

$$S(\omega) = F^{-1}(\omega) \mathbf{P} F^{-H}(\omega) \quad (5)$$

where the complex matrices $F(\omega)$ are given by the expression

$$F(\omega) = \mathbf{I} + \sum_{k=1}^p A_k \exp(-i\omega k) \quad (6)$$

where i is the imaginary number, \mathbf{I} is the unit $(m \times m)$ matrix, and ω is frequency.

Since the matrix $S(\omega)$ is Hermitian and positive semi-definite, its eigenvalues are real and nonnegative. Let us introduce the notation

$$0 \leq \lambda_m(\omega) \leq \dots \leq \lambda_2(\omega) \leq \lambda_1(\omega) \quad (7)$$

for eigenvalues of the matrix $S(\omega)$ ordered in decreasing order, i.e., λ_1 and λ_m denote the maximum and minimum eigenvalues, respectively.

The objects of further study in the proposed approach are frequency-dependent functions $\lambda_i(\omega)$ computed in sequential time windows of length L readings taken with a mutual shift ΔL ($1 \leq \Delta L \leq L$) [Lyubushin, 1993].

Let Δt be a sampling interval of the monitoring system. We choose the coordinate of the right window termination as the parameter τ

$$\tau = \tau_0 + \Delta t(L - 1 + (j - 1)\Delta L) \quad (8)$$

where $j = 1, 2, \dots$ is the number of the time window, and τ_0 is the start of observations. Such a choice of parameter τ is directed toward using values of $\lambda_i(\tau, \omega)$ for predictions: if an anomaly appears in their behavior, then it precedes the time marker τ .

The range of the change in frequency ω in (5) is dictated by the selection of values Δt and L

$$2\pi/((L - 1)\Delta t) \leq \omega \leq \pi/\Delta t \quad (9)$$

From the set of the functions (7) we can combine different statistics that are of interest for monitoring problems. For example, with the exception of the first eigenvalue $\lambda_1(\omega)$, it may be of interest to consider the smallest eigenvalue $\lambda_m(\omega)$ and the ratio

$$\kappa(\omega) = \lambda_1(\omega)/(\lambda_1(\omega) + \dots + \lambda_m(\omega)), \quad 0 < \kappa(\omega) \leq 1$$

which is a measure of the information content of the first principle component. However, we focus below on the quantity $\lambda_1(\omega)$ only, since it is easier to interpret changes in its value than changes in one of the other eigenvalues or their combinations.

Analysis of the Dependencies $\lambda_1(\tau, \omega)$

An increase in the value of $\lambda_1(\tau, \omega)$, i.e., the synchronization of the changes in different components of the vector series $\mathbf{X}(t)$, may be caused by the following situations: (1) the presence of an external noise source with a spatial correlation range which affects all the measurement points; (2) consolidation of the crustal material in the area covered by the monitoring net; and (3) post-seismic variations of geophysical fields after large earthquakes (in seismically active regions).

Reason 1 can be eliminated using multidimensional compensation of noise, allowing for measurement at each monitoring point [Lyubushin, 1993; Lyubushin and Latynina, 1993]. The natural variation in atmospheric

pressure is the main source of broadband, strongly spatially correlated noise. Application of adaptive procedures for compensation of the barometric variations enabled them to be interpreted not only as noise, but also as a unique sounding signal in the low-frequency range, a signal having a response function whose evolution can be used for estimating a change in the upper crustal state. The works by Lyubushin and Malugin [1993] and Lyubushin et al. [1992] give a visual representation of the evolution of the amplitude frequency transfer function from atmospheric pressure variations to both crustal deformations and underground water level in the water-saturated horizons of the aseismic regions (Obninsk and Moscow region). This enabled a number of nontrivial effects to be found, in particular, the quasi-periodic evolutionary regime of the response function for linear deformations (with a period of about 1.5 months) [Lyubushin et al., 1992] and weakening of the upper crustal layers under high-frequency barometric variations (with periods of $T < 10$ hours) [Lyubushin and Malugin, 1993].

Another contribution to the external noise sources described in reason 1 above may be narrowband tidal deformations of the crust, with "correlation radius" equal to the Earth's diameter. To remove this contribution, the following procedure is recommended. After rewriting as a discrete series, harmonics of the two bands where tidal action is concentrated [1/27, 1/23] and [1/13, 1/11] hours⁻¹ are eliminated from both the studied signal and noise using narrowband frequency filtration, and only then is further processing performed. The process of rejecting narrowband tidal noise suppresses information in these bands, but the use of parametric methods (with comparatively small numbers of parameters) in estimating the spectral matrices and response functions permits estimates to be interpolated from adjacent frequency ranges to the rejected bands [Lyubushin, 1993; Lyubushin and Malugin, 1993; Lyubushin et al., 1992].

From the geophysical point of view, the most interesting signal is the synchronization of signals at different monitoring points due to consolidation of small blocks of the crust and a corresponding increase in cohesive forces at their boundaries (reason 2). This reflects the internal dynamics of geological structures [Lyubushin, 1993]. In particular, crustal consolidation can be considered an earthquake precursor since, for energy to be accumulated without loss during many small events, the preparation range must be something of a whole (unified) sort [Lyubushin, 1987, 1991]. Separation of the signal (2) with determination of frequency ranges where the significant deviations of the statistics $\lambda_1(\tau, \omega)$ are observed (i.e., determination of the characteristic frequencies of the medium at the observation point) and comparison of the time intervals τ of the recorded de-

viations with seismic events appear to be the principle target of low-frequency monitoring in seismically active regions. In this way, fundamentally new precursors of earthquakes may be discovered. Study of the $\lambda_1(\tau, \omega)$ statistics with respect to detection of signal 2 is of interest also in monitoring aseismic regions where “hidden” geological activity proceeds (“quiet” earthquakes, creep, reconsolidation processes of small blocks in the Earth’s crust, responses to human industrial activity).

The function $\lambda_1(\tau, \omega)$ is not always characterized by significant peaks well isolated from background variations. This may be a consequence of either the low sensitivity of pickups of the original information or the unsuccessful selection of measured values. Moreover, regularities of interaction between geological structures can be manifested by a moderate increase of $\lambda_1(\tau, \omega)$ in the vicinity of a frequency set rather than by an appearance of a strong maximum in the neighborhood of one frequency. In any case, a pattern recognition technique [Duda and Hart, 1976] can be applied when merely visual analysis of the statistic $\lambda_1(\tau, \omega)$ is troublesome. For this we consider the vector sequence

$$\mathbf{Z}^{(\tau)} = (z_1^{(\tau)}, \dots, z_n^{(\tau)}), \quad z_j^{(\tau)} = \lambda_1(\tau, \omega_j) \quad (10)$$

$$j = 1, \dots, n$$

where ω_j is a collection of the characteristic frequencies satisfying (9).

The vector cloud $\{\mathbf{Z}^{(\tau)}\}$ thus obtained can be analyzed either to separate compact groups (cluster analysis), each of which reflects a certain state of the observation system, or to determine decisively when the observation system is in the “critical” zone preceding geological disasters (earthquake, rock shock, etc). The latter case requires collection of an observation series including several catastrophes so that the cloud $\{\mathbf{Z}^{(\tau)}\}$ contains both “dangerous” (before the catastrophe) and “safe” or “background” vectors $\mathbf{Z}^{(\tau)}$ which makes it conducive to the application of $\{\mathbf{Z}^{(\tau)}\}$ learning algorithms of discriminant analysis [Duda and Hart, 1976]. In both cases the separated compact clusters or dangerous and “safe” ranges of vector locations $\mathbf{Z}^{(\tau)}$ will correspond to some “modes” of the process of consolidation and deconsolidation of the crust [Lyubushin, 1987, 1991].

Postseismic variations in geophysical fields are an additional source of synchronization of records at various sites in the monitoring net in seismically active regions ((3) above). We note that if the primary information pickups of the observation system have low sensitivity (which is expressed in a prolonged “plateau” of constant measured values), then the signal can be a unique synchronizing signal, since a sufficiently high sensitivity is required for the signal to be recorded. Nevertheless,

the signal can also serve as the source of information on events leading to future large earthquakes. This is because we can trace signals corresponding to events leading to a large earthquake (for example, a regular increase in sharp deviations from the statistics $\lambda_1(\tau, \omega)$ in a sequence of events) based on the intensity of responses to past small and moderate earthquakes.

Example of Real Data Processing

Synchronous data from a spatial, low-frequency geophysical monitoring net are still rare, at least for the territory of the former USSR. The principle difficulties encountered in reaching the desired functioning of similar systems include the requirement of continuous and prolonged recording (from several months to several tens of years); long-term stability of pickups related mainly to atmospheric and meteorologic factors; and the requirement of sufficient sensitivity of the pickups (which, as a rule, is contrary to durable stability). None of the observation systems known to the author simultaneously satisfies all of these requirements. As a rule, continuous functioning instruments works only for a small number of observation points or recorded processes (one or two) or for a very large sampling interval Δt . The other frequent pitfall in durable observation systems is the low frequency of primary information pickups.

The data used for illustration of the algorithm operation were provided by G. N. Kopylova (Institute of Volcanology, Petropavlovsk-Kamchatskiy). These data refer to a set of boreholes in the Petropavlovsk geodynamic proving ground, where measurements are currently collected on underground water temperature, output, and concentration of chemical substances and gasing intensity [Kopylova, 1992]. These data are not without shortcomings (e.g., low sensitivity and a large Δt value) but they also have doubtless advantages, including a long observation interval (from 1979 to the present) [Kopylova, 1992], which enables the frequency-time analysis to be carried out in the low-frequency range (on the order of 1 year⁻¹).

Presented in Figures 1, 2, and 3 are the results of processing a very small part of the time series from the Petropavlovsk proving ground (detailed data processing with a wide description of the proving ground will be considered in the next publication): Figure 1 represents the time series of the concentration of Cl⁻ in four boreholes; Figure 2 represents the time series of the concentration of H₄SiO₄ in the same boreholes; and Figure 3 represents the 10-dimensional time series consisting of the components water output, water temperature, and concentration of the following species: Ar, HCO₃⁻, CH₄, Cl⁻, CO₂, H₄SiO₄, He, and N₂ in one of the boreholes.

Figures 1a, 2a, and 3a depict the evolution of the first

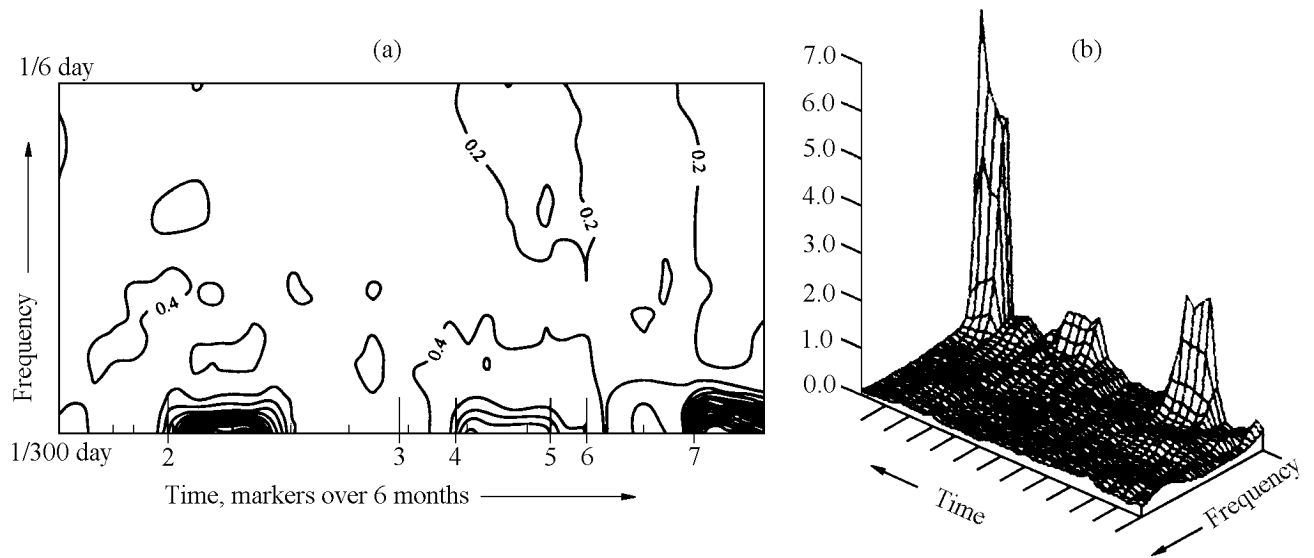


Figure 1.

eigenvalue of the spectral matrix of the corresponding time series (i.e., the dependence $\lambda_1(\tau, \omega)$) in the form of the level lines. Figures 1b, 2b, and 3b show the same dependence in the form of three-dimensional surfaces which allow the scale of variations to be seen quickly. The length of the samples is 821 readings, the record begins on January 3, 1986, and the sampling interval Δt is 3 days. The time window length is $L = 100$ readings (300 days), and the shift of adjacent windows is $\Delta L = 20$ readings (60 days) which resulted in 37 sequential crossing intervals. Before estimating the spec-

tral matrix, operations 1, 2, and 3, were made with the scalar components in each time window. The estimate of the spectral matrix was computed from (5) where the autoregression order was set $p = 3$. The autoregression order was selected by way of sorting the values of p from 1 to 10, comparing the results between them, and choosing the minimal value of p at which all the large-scale features of the $\lambda_1(\tau, \omega)$ behavior are evident. The choice of the order of autoregression is a difficult compromise between stability (small p) and sensitivity (large p) of the estimate [Marple, 1990]. The time axis

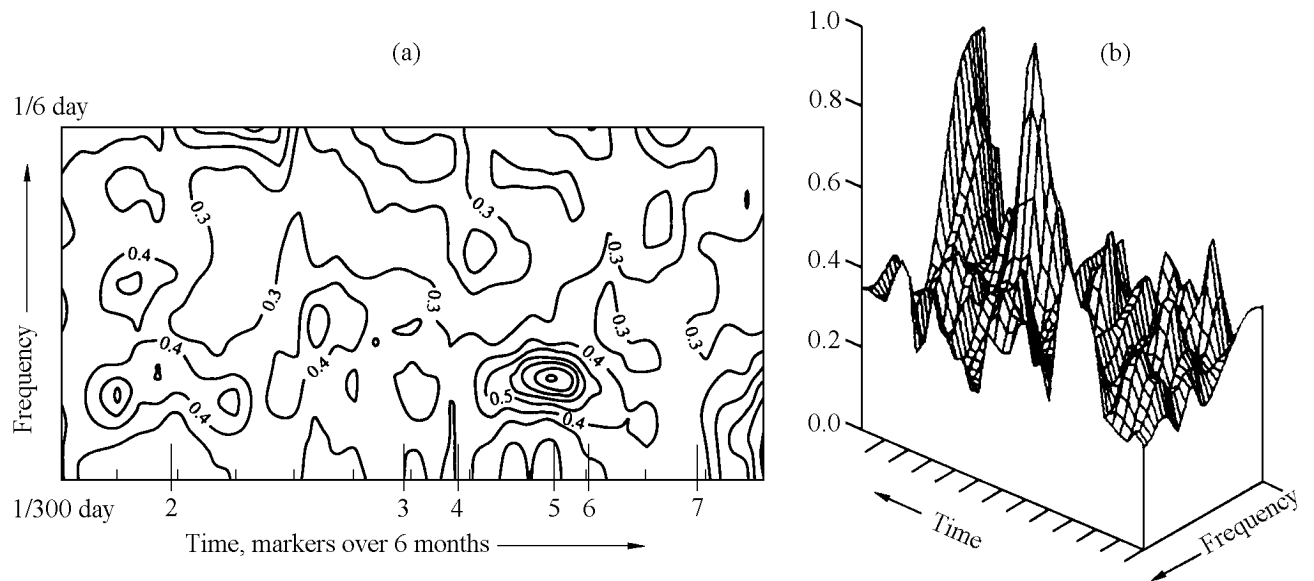


Figure 2.

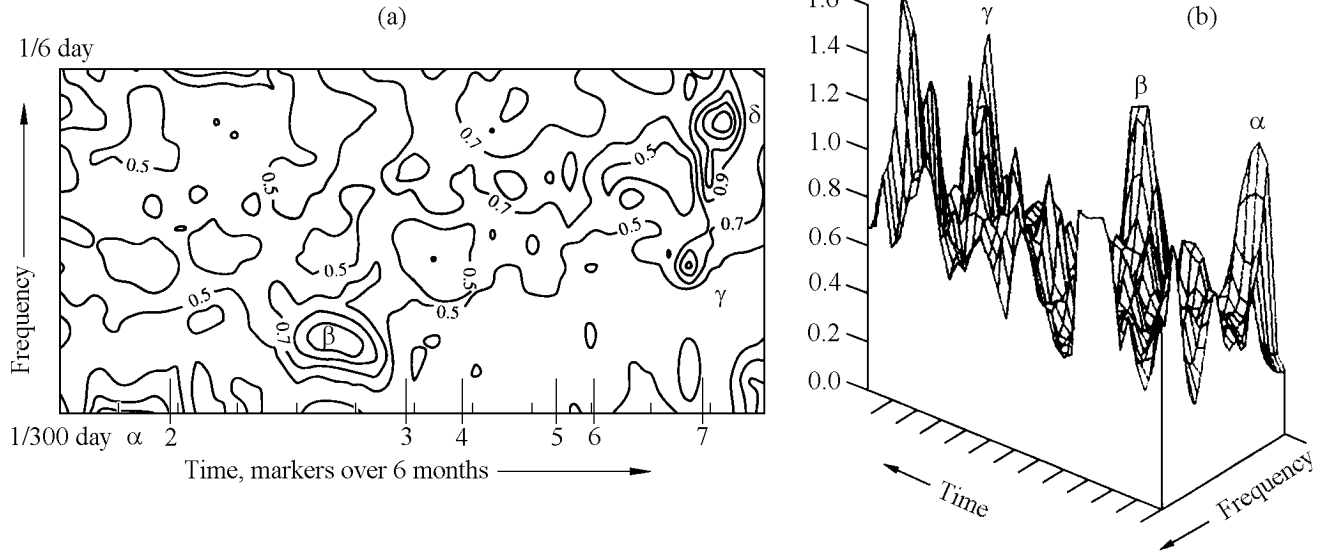


Figure 3.

corresponds to coordinates of the right-hand termination of the window which result in “disappearance” of the first $L = 100$ readings.

Table 1 gives parameters of seven sufficiently large earthquakes occurring near the proving ground during the observation period. The characteristic size of the proving ground is about 50 km, and the distance of hypocenters from the “center” of the proving ground varies from 105 (for event 3) to 170 km (for event 7) [Kopylova, 1992].

On the time axis of Figures 1a, 2a, and 3a the long ticks indicate the earthquakes listed in Table 1. The first earthquake is not plotted, since it belongs to the first window, but the time axis represents the right-hand terminations of the sliding time windows.

Table 1.

	No.					
Date	of day	Magni-	Latitude,	Longitude,	Depth,	
	beginning	tude	degrees	degrees	km	
	of 1986		N.	E.		
1	17.06.86	168	5.0	53.78	160.66	40
2	06.10.87	644	6.6	52.85	160.24	34
3	15.09.89	1354	4.9	53.19	160.01	44
4	01.03.90	1521	5.8	53.29	160.23	24
5	19.12.90	1814	6.1	52.77	160.65	24
6	08.04.91	1924	4.7	52.36	158.21	139
7	02.03.92	2253	7.1	52.82	159.99	40

Let us consider Figure 1. We see here three significant peaks of the $\lambda_1(\tau, \omega)$ function in the low-frequency range. Comparing them with the times of earthquake occurrence, we conclude that they refer to the signal corresponding to synchronization of the postseismic movements after the events 2, 4, and 7. In addition, it should be noted that the convergence of the level lines to a peak begins somewhat earlier than the events themselves: approximately 2 weeks for events 2 and 4 and 1 month for event 7, i.e., we observe a weak signal, corresponding to 2 above transforming into a signal corresponding to 3.

In Figure 2 we see two significant peaks referring completely to signals of the type 3 described above. The first peak is after event 4 and the second one occurs after event 7. It should be noted that the dominant periods are about 3 weeks for the first peak and about 1 month for the second one. The visual analysis of other variations of the $\lambda_1(\tau, \omega)$ dependence has been hampered, but the use of the pattern recognition techniques in the given case is not very because of the small number of estimates for $\lambda_1(\tau, \omega)$ (37 values of the τ parameter over intervals with great overlap, i.e., the number of independent vectors in the set (10) is small).

Figure 3 represents the most complicated picture of variations of the function $\lambda_1(\tau, \omega)$. We note four peaks rising above the general background level. These are symbolized by letters $\alpha, \beta, \gamma,$ and δ and have dominant periods of 300 days, 25 days, 14 days, and 7 days, respectively. It is interesting to note that with time, the peaks migrate to higher frequencies i.e., synchronization is observed on increasingly shorter-period variations. If we were to compare these peaks with the seismic regime, then the $\alpha, \beta,$ and γ maxima can be referred to signals

of type 2 (forerunner synchronization): α is before event 2, β is before events 3 and 4, and γ is before event 7. The sharp deviation δ refers instead to signals of type 3 (postseismic synchronization following event 7).

Conclusions

The approach to decoding synchronization records of different geophysical fields and/or at different geophysical monitoring sites was proposed earlier [Lyubushin, 1993] with emphasis on the frequency bands and time intervals in which the collective behavior of movements is observed. In the present work we modify and describe the implementation of this approach using computers and relying on parametric estimation algorithms based on multidimensional autoregression models.

A classification scheme is presented for synchronization signal types 1, 2, and 3 with a separated forerunner signal (2). In the case when there are difficulties with visual analysis of the frequency-time evolution of the first eigenvalue of the spectral matrix, we recommend the application of cluster analysis and learning discriminant analysis (pattern recognition).

As an example of the application of the algorithm to estimation of the maximum eigenvalue of the spectral matrix, three multidimensional time series of hydrochemical data from Kamchatka were processed. The frequency-time evolution was compared with the seismic regime, and the forerunner (2) and postseismic (3) synchronization signals were decoded.

The computer technique developed for estimating and visualizing the eigenvalues (and their functionals) of the spectral matrices from a multidimensional time series obtained using geophysical monitoring systems can be applied qualitatively to search for new precursors of earthquakes (in seismically active regions) and to investigate background processes in aseismic regions.

Acknowledgments. The work was supported by the Russian Fund for Basic Research (grant 94-05-16120).

References

- Brillindjer, D., *Time Series: Data Processing and Theory*, 536 pp., Mir, Moscow, 1980.
- Duda, R., and P. Hart, *Pattern Recognition and Scene Analysis*, 511 pp., Mir, Moscow, 1976.
- Kopylova, G. N., Analysis of seismic effects on the regime of the Pinachevskiy thermomanifestations in Kamchatka (from observations during 1979–1988), *Vulkanol. Seysmol.*, 2, 3–18, 1992.
- Lyubushin, A. A., Jr., Multidimensional analysis of time series from geophysical monitoring systems, *Izv. AN SSSR. Fizika Zemli*, 3, 103–108, 1993.
- Lyubushin, A. A., Jr., Hierarchic model of seismic process, *Izv. AN SSSR. Fizika Zemli*, 11, 43–52, 1987.
- Lyubushin, A. A., Jr., Model of seismic processes in a block medium, in *Sovremennye Metody Interpretatsiyi Seysmologicheskikh Danykh, Vychislitel'naya Seysmologiya*, vol. 24, pp. 50–61, Nauka, Moscow, 1991.
- Lyubushin, A. A., Jr., V. I. Osika, V. A. Pchelintsev, and L. S. Petukhiva, Analysis of crustal response to atmospheric pressure variations, *Izv. AN SSSR. Fizika Zemli*, 2, 81–89, 1992.
- Lyubushin, A. A., Jr., and L. A. Latynina, Compensation of meteorologic noise in deformation observations, *Izv. AN SSSR. Fizika Zemli*, 3, 98–102, 1993.
- Lyubushin, A. A., Jr., and V. A. Malugin, Statistical analysis of underground water response to the atmospheric pressure variations, *Izv. AN SSSR. Fizika Zemli*, 12, 74–80, 1993.
- Marple, S. L., Jr., *Digital Spectral Analysis and its Application*, 584 pp., Mir, Moscow, 1990.

(Received September 2, 1993.)